



72<sup>nd</sup> Conference of the Italian Thermal Machines Engineering Association, ATI2017, 6–8 September 2017, Lecce, Italy

## Numerical Investigation of High Enthalpy Flows

Francesco Bonelli<sup>a,\*</sup>, Michele Tuttafesta<sup>b</sup>, Gianpiero Colonna<sup>c</sup>, Luigi Cutrone<sup>d</sup>,  
Giuseppe Pascazio<sup>a</sup>

<sup>a</sup>*DMMM & CEMeC, Politecnico di Bari, via Re David 200, 70125, Bari, Italy*

<sup>b</sup>*Liceo Scientifico Statale “L. da Vinci”, Via Cala dell’Arciprete 1 - 76011 Bisceglie (BT), Italy*

<sup>c</sup>*CNR-IMIP, via Amendola 122/D - 70126 Bari (Italy)*

<sup>d</sup>*Centro Italiano Ricerche Aerospaziali (CIRA), Capua, 81043, Italy*

---

### Abstract

This work deals with fluid dynamic simulations of high enthalpy flows. Thermochemical non-equilibrium, typical of such flows, was modelled by using the well known multi-temperature model developed by Park. The non-equilibrium model was implemented in a 2D finite volume solver of the Euler equations and was assessed by comparing the results with available experimental measurements. Several test cases concerning 2D and axisymmetric expansion nozzles were performed by varying gas composition and stagnation temperature.

© 2017 The Authors. Published by Elsevier Ltd.

Peer-review under responsibility of the scientific committee of the 72<sup>nd</sup> Conference of the Italian Thermal Machines Engineering Association

*Keywords:* Non-equilibrium model, multi-temperature, nozzle;

---

### 1. Introduction

The analysis of high enthalpy flows is important for several engineering applications such as atmospheric entry problems, hypersonic transcontinental flights [1], combustion, flows through exhaust valves etc. Moreover, this subject is also relevant for fundamentals physics.

One of the main issue in modelling high enthalpy flows is that the relaxation time of internal states and chemical reactions can be comparable with the fluid dynamic characteristic time, making the flow a system in thermochemical non-equilibrium. One of the most popular approaches to thermochemical non-equilibrium is the multi-temperature model proposed by Park [2]. Such model assigns a single temperature to translational and rotational degrees of freedom (translational temperature), on the other hand, a different temperature (vibrational temperature) is assigned to vibrational levels which are supposed to follow a Boltzmann distribution and evolve according to a Landau-Teller

---

\* Corresponding author. Tel.: +390805963221 ; fax: +390805963411.

E-mail address: [bonellifra@alice.it](mailto:bonellifra@alice.it)

law. Moreover, reaction rate coefficients are supposed to follow the semiempirical Arrhenius law with a controlling temperature that is a weighted geometrical mean of translational and vibrational temperatures.

The aim of the present work is to assess the capability of the Park's model [2] and to investigate non-equilibrium effects in expansion nozzles. To this end, the Park's model for a neutral air mixture was integrated in a 2D finite volume solver of the Euler equations [3, 4]. Such model involves five neutral species, i.e.,  $N_2$ ,  $O_2$ ,  $NO$ ,  $N$ ,  $O$ , which evolve following a kinetic mechanism of 17 reactions, and it considers three vibrational temperatures (one for each molecule).

The model was assessed by considering the experimental setup of Sharma and Ruffin [5], which deals with a high enthalpy nitrogen flow in a 2D nozzle. Moreover, a study of non-equilibrium effects by varying gas composition, stagnation temperature, and geometry configuration was also performed.

The work is organized as follow: in Section 2.1 the governing equations are presented. Then in Section 2.2 the Park's model implemented in this work is described. In Section 2.3 the numerical approach is summarized. The results are presented in Section 3. Finally, the conclusions are summarized.

## 2. Fluid dynamic model

### 2.1. Governing Equations

The flow field was simulated by solving the 2D Euler equations for a multicomponent mixture of reactive gases which in integral vector form read

$$\frac{\partial}{\partial t} \int_{V_0} \mathbf{U} dV + \oint_{S_0} \mathbf{F} \cdot \mathbf{n} dS = \int_{V_0} \mathbf{W} dV. \quad (1)$$

The vector of unknown conserved variables, the fluxes along  $x$  and  $y$  directions and the source term are defined as follows:

$$\mathbf{U} = [\rho_1, \dots, \rho_S, \rho u, \rho v, \rho e, \rho_1 \varepsilon_{vib,1}, \dots, \rho_M \varepsilon_{vib,M}]^T, \quad (2)$$

$$\mathbf{F} = (\mathbf{F}_x, \mathbf{F}_y), \quad (3)$$

$$\mathbf{F}_x = [\rho_1 u, \dots, \rho_S u, \rho u^2 + p, \rho uv, (\rho e + p)u, \rho_1 \varepsilon_{vib,1} u, \dots, \rho_M \varepsilon_{vib,M} u]^T, \quad (4)$$

$$\mathbf{F}_y = [\rho_1 v, \dots, \rho_S v, \rho uv, \rho v^2 + p, (\rho e + p)v, \rho_1 \varepsilon_{vib,1} v, \dots, \rho_M \varepsilon_{vib,M} v]^T, \quad (5)$$

$$\mathbf{W} = [\dot{\omega}_1, \dots, \dot{\omega}_S, 0, 0, 0, \dot{\omega}_{vib,1}, \dots, \dot{\omega}_{vib,M}]^T, \quad (6)$$

where  $\rho_s$  is the gas density of the species  $s$ ,  $S$  is the total number of species,  $p$  is the gas pressure,  $u$  and  $v$  are the flow velocity component, respectively in the  $x$  and  $y$  directions,  $e$  is the specific total energy,  $\varepsilon_{vib,m}$  is the specific vibrational energy of molecule  $m$  and  $M$  is the total number of molecules. The total density is given by  $\rho = \sum_s \rho_s$ .  $\{\dot{\omega}_s\}$  are the chemical source terms, whereas  $\{\dot{\omega}_{vib,m}\}$  are the vibrational energy source terms.

A relation between  $p$  and  $e$  is employed to close the system (1) [6]

$$p = (\bar{\gamma} - 1) \left[ \rho e - \rho (\varepsilon_{vib} + \varepsilon_{chem}) - \rho \frac{u^2 + v^2}{2} \right], \quad (7)$$

where  $\bar{\gamma}$  is the specific heats ratio of the gas mixture,  $\varepsilon_{vib}$  and  $\varepsilon_{chem}$  are the total contribution of vibrational and chemical energies given by

$$\varepsilon_{vib} = 1/\rho \sum_{s=1}^M \rho_m \varepsilon_{vib,m}, \quad (8)$$

$$\varepsilon_{chem} = 1/\rho \sum_{s=1}^S \rho_s h_s^f, \quad (9)$$

where  $h_s^f$  is the formation enthalpy per unit mass of species  $s$ . More details can be found in Refs. [4, 6].

## 2.2. Park's thermochemical model

For a five species neutral air mixture the Park model considers a total of 17 reactions, i.e., 15 dissociation reactions (five for each molecule)



where X is the generic collision partner, i.e., N<sub>2</sub>, O<sub>2</sub>, NO, N or O, and two Zeldovich (exchange) reactions



The chemical source terms  $\{\dot{\omega}_s\}$  were evaluated by using the law of mass action

$$\dot{\omega}_s = M w_s \sum_{i=1}^{N_r} \nu_{si} RR_i, \quad (15)$$

where  $N_r$  is the number of reactions,  $M w_s$  is the molecular weight of the species  $s$ ,  $\nu_{si}$  is the difference between the product and reactant stoichiometric coefficients of the species  $s$  in the  $i^{\text{th}}$  reaction and  $RR_i$  is the reaction rate of the  $i^{\text{th}}$  reaction given by

$$RR_i = k_{f_i} \prod_{s=1}^S C_s^{\nu'_{is}} - k_{b_i} \prod_{s=1}^S C_s^{\nu''_{is}}, \quad (16)$$

where  $k_{f_i}$  and  $k_{b_i}$  are the forward and backward reaction rate coefficients,  $\nu'_{is}$  and  $\nu''_{is}$  are the reactant and product stoichiometric coefficients of the species  $s$  in the  $i^{\text{th}}$  reaction and  $C_s$  is the molar concentration of the species  $s$ . Forward rate coefficients follow a semiempirical Arrhenius law

$$k_{f_i} = A_i T_x^{n_i} \exp\left(-\frac{T_{d_i}}{T_x}\right), \quad (17)$$

where constants  $A_i$ ,  $n_i$  and  $T_{d_i}$  are given in Ref. [2, p. 326] [7]. Following Park [2, p. 138] [7], the controlling temperature  $T_x$  is the translational temperature ( $T$ ) for the Zeldovich (exchange) reactions whereas a geometrically averaged temperature in the case of dissociation reactions, i.e.,

$$T_{am} = T_{V_m}^q T^{1-q}, \quad (18)$$

where  $T_{V_m}$  is the vibrational temperature of molecule  $m$  and  $q$  is a parameter here assumed equal to 0.5. In the present work a separate  $T_{V_m}$  was considered for each molecule, solving the corresponding energy transport equation. Forward and backward reaction rate coefficients are connected by the equilibrium constant,

$$K_{eq_i} = \frac{k_{f_i}}{k_{b_i}}, \quad (19)$$

whose expression are given in Ref. [2, p. 35].

The vibrational energy source term of molecule  $m$   $\{\dot{\omega}_{vib,m}\}$  is written as the sum of a collisional  $\{\dot{\omega}_{LT,m}\}$  and a chemical  $\{\dot{\omega}_{chem,m}\}$  part [2, p. 125].

The collisional term follows the Landau-Teller equation

$$\dot{\omega}_{LT,m} = \rho_m \frac{\varepsilon_{vib,m}(T) - \varepsilon_{vib,m}(T_{V_m})}{\tau_m}, \quad (20)$$

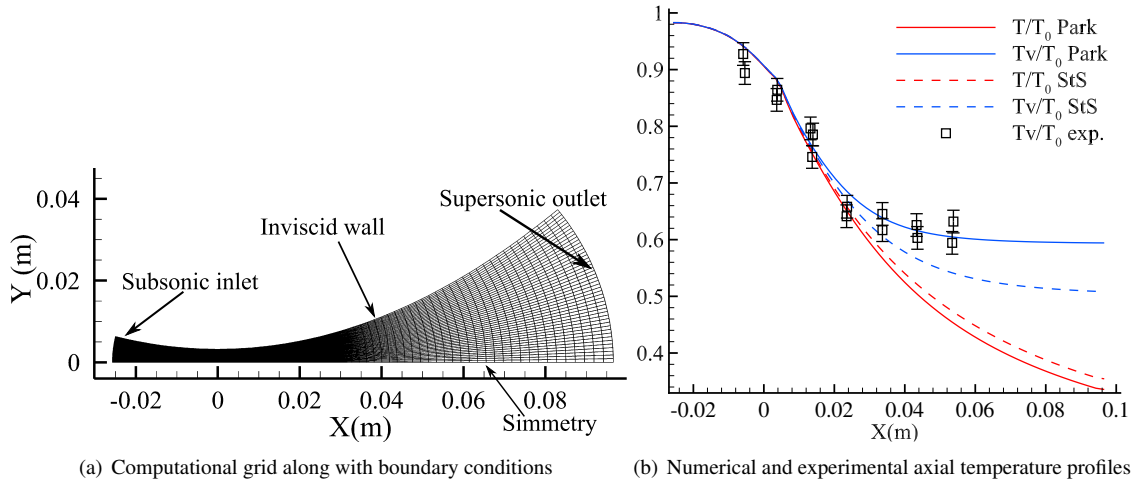


Fig. 1. Sharma and Ruffin [5] test case:  $65 \times 47$  fluid cells computational grid along with boundary conditions (a). Numerical and experimental axial temperature profiles (b).

where  $\varepsilon_{vib,m}(T)$  is the vibrational energy at equilibrium and  $\tau_m$  is the relaxation time evaluated with the Millikan-White expression [8] [2, p. 58] [7] plus a correction for high temperatures [2, p. 60] [7].

The chemical  $\{\dot{\omega}_{chem,m}\}$  contribution reads [2, p. 107, 126]

$$\dot{\omega}_{chem,m} = \frac{D_m}{2} \dot{\omega}_m, \quad (21)$$

where  $D_m$  is the dissociation energy per unit mass of molecule  $m$ .

Finally, the harmonic oscillator model is used to evaluate vibrational energies

$$\varepsilon_{vib,m} = \frac{R_m \theta_m}{\exp(\theta_m/T_{V,m}) - 1}, \quad (22)$$

here  $\theta$  is the characteristic vibrational temperature equal to 3393 K, 2273 K and 2739 K for the  $N_2$ ,  $O_2$  and NO molecules, respectively [2, p. 123]. Further details can be found in Ref. [4].

### 2.3. Numerical method

The system of governing equations (1) is solved by using an operator-splitting procedure [6]. This approach separates the equations into a homogeneous part (non-reactive Euler equations) and one concerning source terms (chemical step). The two systems are thus solved in two successive steps.

In the present implementation, convective fluxes of the homogeneous part can be solved by using either the Steger and Warming flux vector splitting approach [9] or the AUSMPW+ scheme of Kim et al. [10] (here MUSCL method can be used to get higher accuracy). Time integration is entrusted to a two-step 2nd or three-step 3th order Runge-Kutta scheme.

As far as the chemical step is concerned, in order to take into account the stiffness introduced by chemical reactions, a Gauss-Seidel iterative scheme was employed. Here the time step is a fraction of the fluid dynamic one which in turn is evaluated on the basis of the CFL condition. More details on the model are give in Ref. [6].

## 3. Results

In order to assess the accuracy and reliability of the computational model, the well known experimental results obtained in the Electric Arc Shock Tube (EAST) facility at NASA Ames Research Center by Sharma and Ruffin [5] were considered. Such results have already been employed in Ref. [6] to assess a state-to-state (StS) model.

Table 1. Test cases initial conditions. (Based on Ref. [6])

Test cases	Thermochemical inlet conditions ( $T_0 = 5600$ K, $T_{V_m} = 5600$ K, $P_0 = 100$ atm)	
(1) Nitrogen flow [5]	$N_2$ molar fracion	0.9884
	$N$ molar fracion	0.0116
(2) Oxigen flow	$O_2$ molar fracion	0.2834
	$O$ molar fracion	0.7166
(3) Five species air flow	$N_2$ molar fracion	0.64844
	$O_2$ molar fracion	0.02831
	$NO$ molar fracion	0.08730
	$N$ molar fracion	0.00941
	$O$ molar fracion	0.22653
Thermochemical inlet conditions ( $T_0 = 7000$ K, $T_{V_m} = 7000$ K, $P_0 = 100$ atm)		
(4) Nitrogen flow	$N_2$ molar fracion	0.9063
	$N$ molar fracion	0.0937
(5) Five species air flow	$N_2$ molar fracion	5.8532e-1
	$O_2$ molar fracion	4.8989e-3
	$NO$ molar fracion	4.9202e-2
	$N$ molar fracion	7.5298e-2
	$O$ molar fracion	2.8528e-1
Thermochemical inlet conditions ( $T_0 = 9000$ K, $T_{V_m} = 9000$ K, $P_0 = 100$ atm)		
(6) Nitrogen flow	$N_2$ molar fracion	0.5096
	$N$ molar fracion	0.4904
(7) Five species air flow	$N_2$ molar fracion	3.2610e-1
	$O_2$ molar fracion	5.8082e-4
	$NO$ molar fracion	1.7167e-2
	$N$ molar fracion	3.9227e-1
	$O$ molar fracion	2.6388e-1

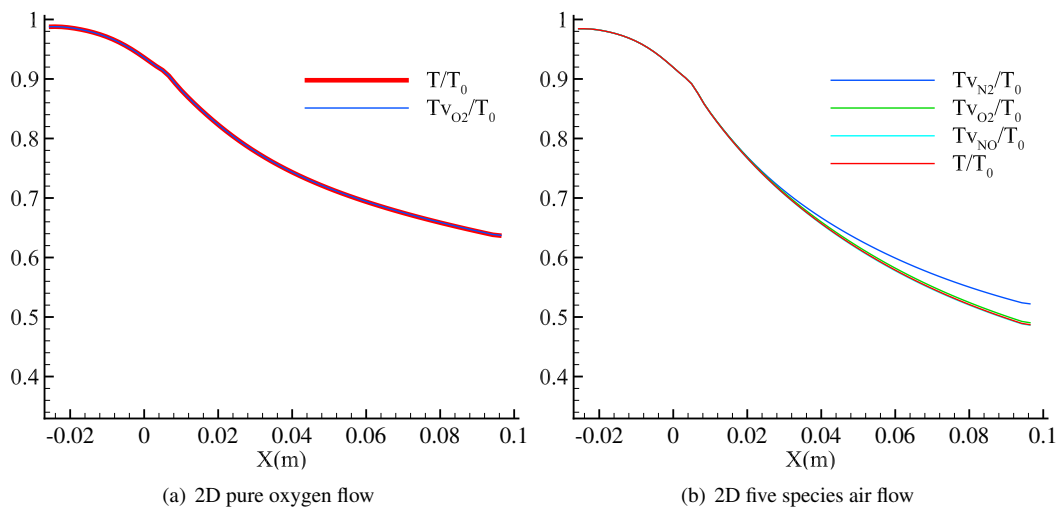


Fig. 2. Normalized axial temperatures profiles for a 2D nozzle with  $T_0 = 5600$  K and  $P_0 = 100$  atm: pure oxygen flow (a); five species air flow (b).

In their work Sharma and Ruffin [5] measured the vibrational relaxation of nitrogen in a 2D expansion nozzle by using the Raman scattering technique. The 2D converging-diverging nozzle has a throat height of 0.64 cm, located at

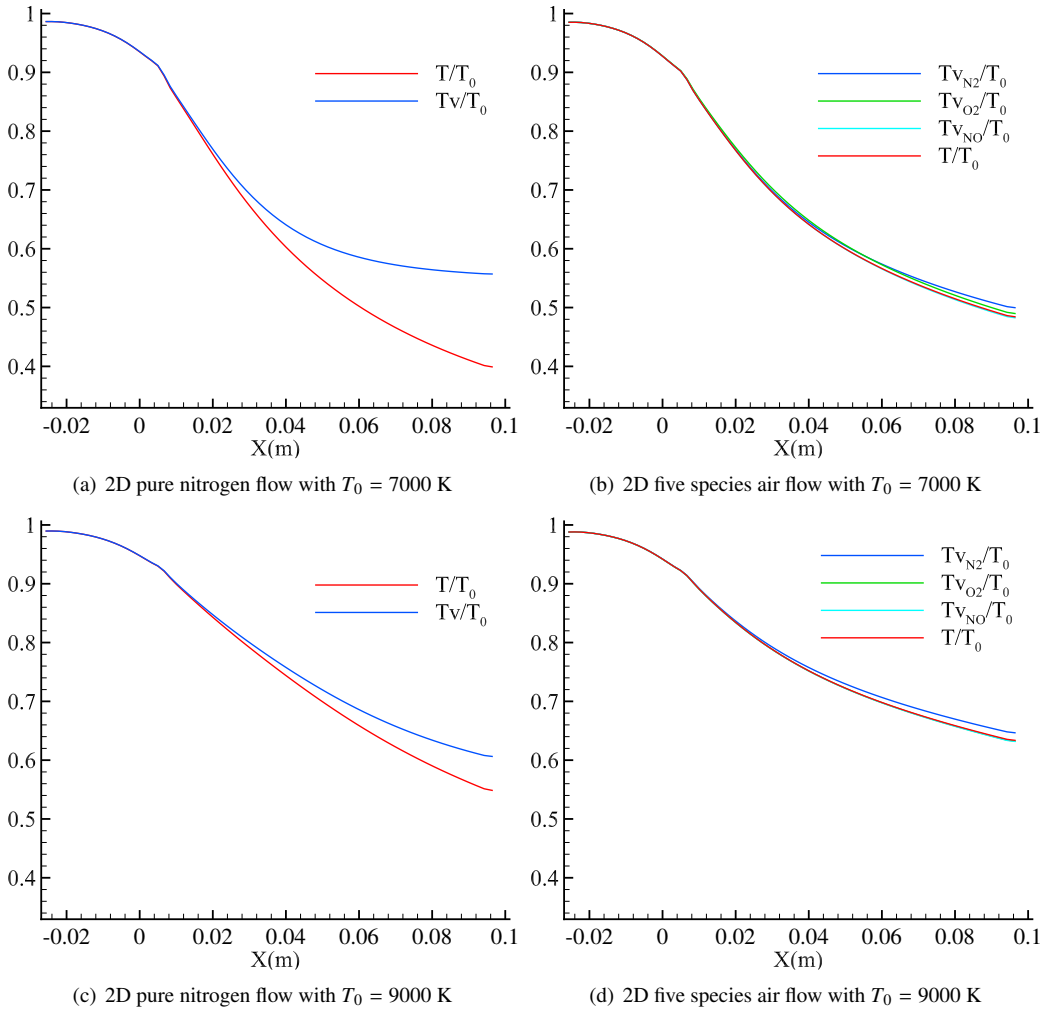


Fig. 3. Normalized axial temperatures profiles for a 2D nozzle flow with  $P_0 = 100$  atm by varying  $T_0$  and gas composition: (a) and (c) pure nitrogen flow with  $T_0 = 7000$  K and  $T_0 = 9000$  K, respectively; (b) and (d) five species air flow with  $T_0 = 7000$  K and  $T_0 = 9000$  K, respectively.

2.5 cm downstream of the stagnation chamber, a total length of 10.8 cm and a width of 10.0 cm. According to Ref. [5], downstream of the throat, the nozzle section area ( $A$ ) follows the law:

$$\frac{A}{A_t} = 1 + \left( \frac{x}{2.54} \right)^2, \quad (23)$$

where  $A_t$  and  $x$  are the section area at the throat and the axial distance from the throat (expressed in cm), respectively. The same law was also used to give the section area of the convergent part. Nitrogen stagnation temperature ( $T_0$ ) and stagnation pressure ( $P_0$ ) are roughly 5600 K and 100 atm, respectively. The same computational setup of Ref. [6] was used. Specifically, exploiting the symmetry condition, half nozzle was simulated by using a structured grid which includes  $65 \times 47$  fluid cells. Convective fluxes were evaluated with the Steger and Warming flux vector splitting scheme. Table 1 and Fig. 1 (a) show the initial condition (test case (1)) and the computational grid along with boundary conditions, respectively.

Fig. 1 (b) shows the numerical axial profiles of the normalized translational and vibrational temperatures obtained in this work and the StS profiles of Ref. [6] along with the experimental measure of the vibrational temperature. The freezing of the vibrational temperature manifests a strong thermal non-equilibrium downstream of the nozzle throat. From a quantitative point of view, the results obtained by using the Park's model show a better agreement with

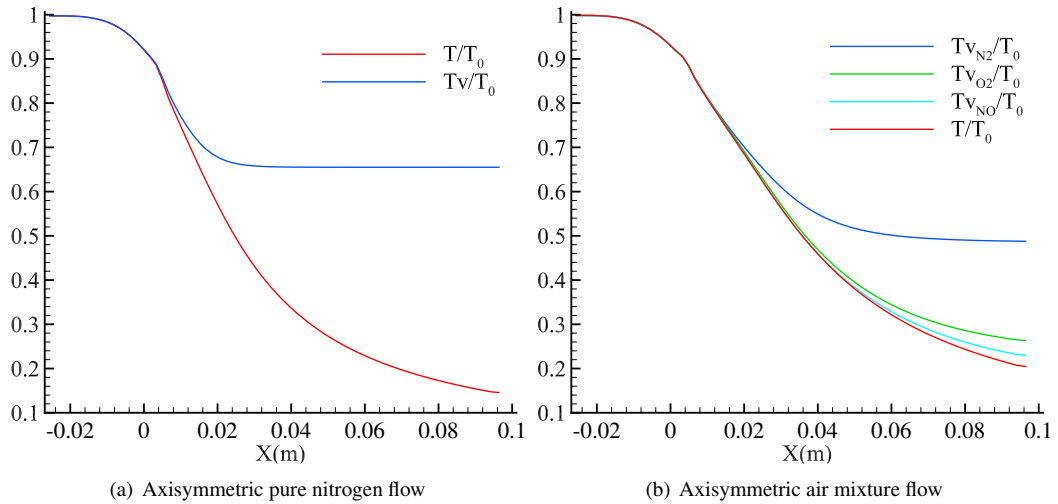


Fig. 4. Normalized axial temperatures profiles for an axisymmetric flow with  $T_0 = 5600$  K and  $P_0 = 100$  atm: pure nitrogen flow (a); five species air mixture flow (b).

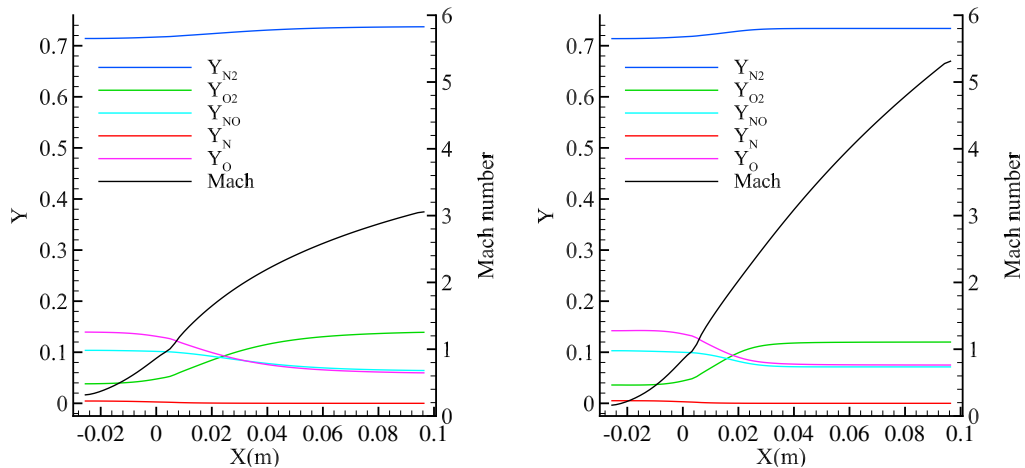


Fig. 5. Mass fraction (Y) and Mach number axial profiles for a five species air mixture flow: 2D (left); axisymmetric (right)

measurements compared to the ones provided by the StS approach. Such behavior is not surprising [5, 11] since the Landau-Teller model was tuned using experimental data [8]. Therefore, for a fair comparison a different test case was considered in Ref. [4] where details of the computational cost are also provided.

In order to investigate gas composition effects, the same computational setup was used by considering a pure oxygen flow and a five species air mixture flow. Initial condition are summarized in Table 1 (test cases (2) and (3)). The results in terms of translational and vibrational temperatures along the axis are given in Fig. 2. Due to recombination processes that release energy, temperatures at the nozzle exit are higher with respect to the pure nitrogen flow. Moreover, vibrational temperatures are closer to the translational one (for a pure oxygen flow is exactly the same) thus showing that the relaxation of internal states is much faster.

The effect of stagnation temperature was also investigated by considering two additional  $T_0$ , i.e., 7000 K and 9000 K. Both the pure nitrogen and the five species air mixture were considered (initial condition are given in Table 1, test cases (4), (5), (6) and (7)). The results in terms of normalized axial temperatures given in Fig. 3 show that by increasing  $T_0$  thermal non-equilibrium decreases. Indeed, especially in the case of pure nitrogen, the vibrational temperature approaches the translational one with larger  $T_0$ , thus showing a faster relaxation of internal states.

Finally, the same nozzle profile was used with an axisymmetric condition thus studying a 3D flow but preserving the same computational cost of a 2D one. With an axisymmetric geometry the area ratio of the exit to the throat is larger so higher velocities develop in the divergent part of the nozzle. The stronger expansion causes larger thermochemical non-equilibrium effects. Such effects are evident in Figs. 4 and 5 where the results concerning a pure nitrogen flow and a five species air mixture flow (with  $T_0 = 5600$  K and  $P_0 = 100$  atm) are given in terms of axial profiles of temperatures, mass fractions and Mach number.

As concerns the temperature profiles given in Figs. 4 (a) and (b), vibrational temperatures show a larger freezing of internal states with respect to the same cases studied with a 2D geometry (see Fig. 1 (b) and Fig. 2 (b)).

Figs. 5 (left) and (right) show the results obtained by using both the 2D and the axisymmetric geometry, for a five species air mixture flow, in terms of axial profiles of the species mass fractions and of the Mach number. Both cases show a mass fraction freezing in the divergent part of the nozzle thus proving a strong chemical non-equilibrium effect.

#### 4. Conclusions

The present paper dealt with 2D simulations of high enthalpy flows through converging-diverging nozzles. The Park multi-temperature model, implemented in a 2D solver of the Euler equations, was assessed by comparing the results with the experimental measures of Sharma and Ruffin [5]. In such experiments, obtained in the Electric Arc Shock Tube (EAST) facility at NASA Ames Research Center, the authors measured the nitrogen vibrational temperature by using the Raman scattering technique. Although the Park model is based on simplified hypotheses (a StS model would be a better approach even though it is about three orders of magnitude more time consuming [4, 6]), numerical results showed a good agreement with measurements. Therefore, an investigation on non-equilibrium effects was carried out by varying gas composition, stagnation temperature and geometry configuration. As concern gas composition, the numerical results showed that pure oxygen mixtures and five species air mixtures have a faster relaxation of internal states with respect to a pure nitrogen mixture. Even by increasing the stagnation temperature the internal states seem to relax faster. Finally, the use of an axisymmetric geometry causes larger non-equilibrium effects due to the stronger expansion taking place in the nozzle.

#### Acknowledgements

This research has been supported by grant n. PON03PE-00067-6 APULIA SPACE.

#### References

- [1] Bonelli F, Cutrone L, Votta R, Viggiano A, Magi V. (2011) "Preliminary Design of a Hypersonic Air-breathing Vehicle." *17th AIAA International Space Planes and Hypersonic Systems and Technologies Conference 11–14 April 2011, San Francisco, California, International Space Planes and Hypersonic Systems and Technologies Conferences*. AIAA 2011-2319.
- [2] Park, Chul. (1990) "Nonequilibrium Hypersonic Aerothermodynamics." *John Wiley & Sons*.
- [3] Tuttafesta M, Colonna G, Pascazio G. (2013) "Computing unsteady compressible flows using Roes flux-difference splitting scheme on GPUs." *Computer Physics Communications* 184.6 (2013): 1497–1510.
- [4] Bonelli F, Tuttafesta M, Colonna G, Cutrone L, Pascazio G. (2017) "An MPI-CUDA approach for hypersonic flows with detailed state-to-state air kinetics using a GPU cluster." *Computer Physics Communications* (2017). <https://doi.org/10.1016/j.cpc.2017.05.019>.
- [5] Sharma, SP and Ruffin, SM. (1993) "Vibrational Relaxation Measurements in an Expanding Flow Using Spontaneous Raman Scattering." *J. Thermophys. Heat Transfer* 7.4 (1993): 697–703.
- [6] Tuttafesta M, Pascazio G, Colonna G. (2016) "Multi-GPU unsteady 2D flow simulation coupled with a state-to-state chemical kinetics." *Computer Physics Communications* 207 (2016): 243–257.
- [7] Park, Chul. (1993) "Review of chemical-kinetic problems of future NASA missions, I: Earth entries." *J. Thermophys. Heat Transfer* 7.3 (1993): 385–398.
- [8] Millikan, RC and White, DR. (1963) "Systematics of Vibrational Relaxation." *The Journal of Chemical Physics* 39.12 (1963): 3209.
- [9] Steger, JL and Warming, RF. (1981) "Flux vector splitting of the inviscid gasdynamic equations with application to finite-difference methods." *Journal of Computational Physics* 40.2 (1981): 263–293.
- [10] Kim KH, Kim C, Rho OH. (2001) "Methods for the Accurate Computations of Hypersonic Flows: I. AUSMPW+Scheme." *Journal of Computational Physics* 174.1 (2001): 38–80.
- [11] Cutrone L, Tuttafesta M, Capitelli M, Schettino A, Pascazio G, Colonna G, AIP Conf. Proc. 1628 (2014): 1154–1161.